



Effects of Lateral Constraints and Geometrical Characteristics on Deformation Capacity of the Persian Historic Unreinforced Masonry Shear Walls under Uncertainty Conditions

M. Ghamari^a, M. S. Karimi^{*a}, A. AmirShahkarami^b

^a Faculty of Civil Engineering, Semnan University, Semnan, Iran

^b Department of Civil & Environmental Engineering, Amirkabir University of Technology, Tehran, Iran

PAPER INFO

Paper history:

Received 14 March 2020

Received in revised form 27 April 2020

Accepted 04 August 2020

Keywords:

Unreinforced Masonry Shear Walls

Lateral Constraints

Aspect Ratio

Nonlinear Pushover Analysis

Partial Factor for Deformation Capacity

ABSTRACT

In the most structural codes, deformation capacity of the unreinforced masonry shear walls is estimated based on their structural behavior (failure mode) and aspect ratio. In this paper, deformation capacity was determined for the Persian historic brick masonry walls by considering the effects of various parameters such as lateral constraints, aspect ratio and thickness. Also, to take into account the uncertainties in material and geometry of the walls in their deformation capacity, partial factor γ_{du} was proposed, somehow, deformation capacity of masonry wall is determined by multiplying this factor in the computed deformation. Accordingly, the in-plane behavior of 48 different specimens of masonry walls with four lateral constraint configurations (contribution of transverse walls and also top slab), four distinct aspect ratios (height to length) of 0.5, 0.75, 1.0 and 1.5, three traditional wall thicknesses of 0.20, 0.35 and 0.50 m, under pre-compression load of 0.10 MPa were computed using nonlinear pushover analyses. Then, the obtained force-deformation curves were idealized by bilinear curves (linear elastic – perfectly plastic) to make them easier for comparison objectives as well as to be more adopted in practical purposes. The latter results indicated that deformation capacity of the shear walls decreases by stiffer lateral constraints, more thickening; and decrease in height-to-length aspect ratio. In addition, it was observed that the transverse walls (vertical constraints on two sides, and at two ends of the base shear walls) were more efficient in reducing deformation capacity than the top slab (horizontal constraint). As a result, according to the numerical calculations, the ultimate drift value for the Persian historic brick masonry walls determined between 1.3% and 2.7%. Eventually, the partial factor of γ_{du} to consider uncertainty in modulus of elasticity and thickness assessment in deformation capacity of the Persian historic masonry shear walls achieved in the range of 1.3 to 1.7.

doi: 10.5829/ije.2020.33.11b.02

1. INTRODUCTION

Masonry structures are one of the oldest and most widely used constructions. In Iran, many masonry structures were built using clay units walls and jack-arch top slab (ceiling). Seismic vulnerability is a serious matter for masonry structures and the most vulnerable members during earthquakes are the load-bearing shear walls [1]. One of the main factors in seismic assessment of the masonry shear walls is their deformation capacity, which so far, limited researches has been carried out on this

context [2]. Deformation capacity of masonry shear walls is affected by various factors such as; aspect ratio, thickness, and lateral constraints of the wall, as well as gravitational load level, in addition to the material properties. Because of limited knowledge on deformation capacity of the masonry walls and lack of reliable analytical model, directing a study on this area seemed inevitable. In recent years, some researchers have investigated on behavior of the masonry structures using finite element methods; in which, mostly adopted an identical homogenized properties for the units and

*Corresponding Author Institutional Email: mskarimi@semnan.ac.ir (M. S. Karimi)

mortar; which known as “macro modelling”. In addition, behavioral models of masonry materials with homogeneous properties were developed, ignoring the effects of mortar bonds (while are able to model local failures) [3]. This process led to suggest a nonlinear finite element model for the behavior of masonry materials based on biaxial experiments on masonry assemblages [4]. This model is capable to consider nonlinear effects of materials and also progressive local failures [5]. Loading on masonry walls is mainly applied in two forms of in-plane shear and out-of-plane bending. Due to multi-directionality of the earth motions during earthquake, accurate seismic modeling of the masonry structures should include both in-plane and out-of-plane loads, simultaneously. By locating shear walls perpendicularly, in-plane behavior dominantly controls response of the walls. However, the effect of simultaneous loadings was experimentally studied on smaller wall specimens than the real ones; with different aspect ratios. It was found that aspect ratio had significant effect on behavior of the masonry walls, especially on deformation capacity [6, 7]. This led to consider mainly the in-plane shear loading in numerical modellings, which these conditions was achieved by applying appropriate boundary conditions, laterally, to prevent out-of-plane failure [8]. Simplified equations have also been proposed for shear strength of the masonry walls under different loading conditions (concentrated, distributed and out-of-plane loading) [9]. By research progressing, more completed and simpler relations have been proposed to determine the shear strength of masonry walls on the finite element basis [10]. Furthermore, using analytical methods, behavioral force-deformation curve, based on an elastic-perfectly plastic behavior for masonry materials, was proposed [11, 12].

Transverse wall or flange were defined as part of the out-of-plane wall that participates with the shear wall to resist lateral (out-of-plane) loads [13]. The influence of transverse wall (flange) for unreinforced masonry building (URM) walls under in-plane (shear) loading has been investigated, too. Based on the report NZSEE [14], the in-plane response of URM walls is significantly influenced by the presence of transverse walls. Yi [15] indicated the effects of transverse walls (flanges) on the maximum strength of shear walls, and also noted that no experimental data were available to specifically investigate the URM shear walls with transverse wall. In these investigations, it was determined that the amount of drift depends on the locations of the transverse walls to the in-plane wall. It was also determined that the location of the transverse walls has a significant effect on shear strength of the wall. If the transverse wall is positioned closer to either ends of the wall, its shear strength increases, but when the transverse wall is in the middle of the in-plane wall, it has no effect on its shear strength [16].

The Eurocode 6 [17], Eurocode 8 [18], and several FEMA guidelines [19, 20] debated about drift capacity for URM walls. In Eurocode 8-Part 3 [18], deformation capacity of the masonry structures is dependent on the aspect ratio and the modes of failure. However, the deformation capacity of the shear walls is mainly influenced by their lateral constraints which define the stiffness and strength of the horizontal (top slab) and vertical (transverse wall) constraints. FEMA 306 [19] and FEMA 273 [20] distinguishes drift capacities for different damage levels. The drift capacities proposed by FEMA 306 [20] are very similar to those in Eurocode 8 [18]. Contrary to the aforementioned codes, the Swiss code considers drift capacity as a function of axial stress ratio of the masonry compressive strength [21]. The study on effect of the geometry and aspect ratio (height to length) showed that these parameters had a great effect on shear wall deformation capacity, which increased by decreasing size (i.e. its length) [6]. In recent years, deformation-based methods have been gradually developed for the seismic assessment of existing masonry structures. It is generally accepted that methods of evaluating structural damage based on materials deformation predicts the conditions of damages and their distributions, more realistically [22]. Thus, it would be vital to consider the deformation capacity of masonry structures on their assessing or design. In this regard, the in-plane behavior of several masonry walls with different modes of failure [2] and lateral constraints [23] has been investigated. On the one hand, the existence of significant variability in the experimental data and the lack of a reasonable conclusion for the displacement capacity of the URM shear walls based on the experimental data, and on the other hand, lack of valid analytical model, limits for either the displacement capacity or the force-displacement relationship of URM walls [2]. It should be noted that most of the researches has been done on the strength characteristics of the in-plane response of URM walls. Petri and Bayer [23] studied the effect of boundary conditions on displacement capacity by performing six series tests of static and/or cyclic shear loadings on unreinforced masonry shear walls. Tomazevic and Weiss [24] examined a set of samples with varying aspect ratios and in actual size by shaking table tests to determine the force-reduction factor for the URM structures.

2. RESEARCH APPROACH

In this study, shear walls with four different lateral constraint components were modelled to study the behavior of Persian historic masonry shear walls, influenced by the presence of transverse walls and of a top slab, as illustrated in Figure 1. In the first model, a shear wall was modeled without any lateral component, known as the base wall, as "W" (Figure 1a).

Subsequently, with the gradual increase of the neighboring members, other masonry specimens with different lateral constraints were created. Figure 1b, exposed a specimen with a horizontal component or top slab and is represented by the "H" index. The third set of specimens with transverse walls at two ends and on both sides of the wall is presented in Figure 1c as "V". In the fourth typologies, both the horizontal (top slab) and vertical (transverse walls on both sides) constraints are placed with the base shear wall specimen (Figure 1d), which is named "H+V".

For simulation purposes, masonry materials should be considered as quasi-brittle materials. The SOLID65 element (from the library elements of the ANSYS [25] program) was used to represent the properties of homogeneous composition of bricks and mortar. This is a dedicated three-dimensional solid iso-parametric element to model nonlinear response. The element is a hexahedron with eight nodes, with three degrees of freedom at each node (translations in x, y and z directions) and eight integration points. The walls are restricted by the conditions of presence of the connecting side elements. At borders of the specimens in which there is no connecting side constraint, nodes on those edges of the wall are only prevented from lateral movement. Transition at nodes located on edge borders of the vertical (transverse walls) and/or horizontal (top slab) constraints, are free along the directions located on the wall plane, and the lateral transition, perpendicular to the wall plane, was prevented. This was regarding the point that historic walls are not confined in a frame and are able to displace vertically. To apply support conditions at the base, all nodes of the masonry block elements, located at the base of the wall, were fully fixed.

In this research, the base walls with a constant height of 3.0 m, three thicknesses of 0.20, 0.35, and 0.50 m, and four lengths of 2.0, 3.0, 4.0, and 6.0 m (resulting in height-to-length aspect ratios of 1.5, 1.0, 0.75 and 0.5,

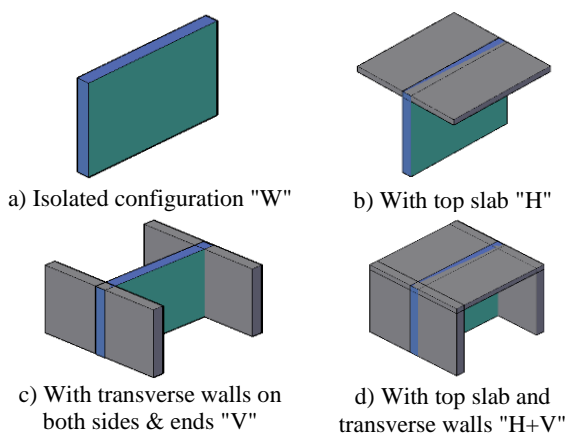


Figure 1. Masonry shear wall models with distinct lateral constraints

respectively) were modelled. The half-lengths of the horizontal component (top slab) and the transverse walls, attached to each side of the main shear wall, is equal to 3.0 m. This value was chosen according to definition of the effective loading span with the maximum distance of two masonry walls i.e. 6.0 m. Thickness of the transverse walls are the same as the base shear wall, in each model. The top slab is also selected from the Persian jack-arch with a thickness of 20 cm. The specimens were analyzed under corresponding gravity load of one floor, only. The gravity load was calculated according to the applied dead-load of 400 kg/m² and live-load of 200 kg/m², of one floor. Hence, the gravity load was 100 kN/m² (0.2 MPa), which applied on the top of the shear walls. In addition, monotonically increasing in-plane shear deformation was applied on the top of the wall, as the shear loading. Newton-Raphson iteration with deformation control and the convergence criterion with a tolerance of 10⁻⁴ was used to run the numerical analyses.

In this research, due to the lack of sufficient knowledge about the effective factors in deformation capacity of the masonry shear walls, it was attempted to determine a partial safety factor for their deformation capacity, using the protocols and techniques available in the structural codes. The partial safety factor for deformation capacity (γ_{du}) is a coefficient that can be used to model uncertainties. To evaluate the safety of historic masonry structures, this study is focused on two parameters, namely the modulus of elasticity and thickness of the wall as input parameters for uncertainty determination. The strength value of the masonry materials is affected by the modulus of elasticity, therefore a correlation with those properties is considered such that they would change accordingly to the changes of the modulus of elasticity. Thickness is another relevant factor in the stiffness and shear strength of the walls.

In this study, ANSYS software [25] was used for the masonry wall specimen analyses under in-plane loading. The characteristics of isotropic homogeneous masonry material used in this study; are presented in Table 1. This table indicates the mechanical properties for the assemblage of clay brick and clay-gypsum mortar; used in Persian historical buildings in Qazvin. These mechanical properties have been determined from the experimental tests [26], and also available in literature [27, 28].

TABLE 1. Mechanical properties for masonry assemblage [27-29]

Bulk density (kg/m ³)	1530
Modulus of elasticity (MPa)	2730
Poisson's ratio (-)	0.17
Compressive strength (f_c) (MPa)	2.73
Tensile strength (f_t) (MPa)	0.27

In general, description of failure criterion for the homogenized masonry material is a complicated task, and it needs to be investigated by the results of several tests, including biaxial tests. In here, the failure criterion used in FE modeling of the masonry materials is the Willam-Warnke failure criterion [29]. This failure criterion is expressed by the multi-axial stress conditions. In this theory, each stress is not individually compared to its limit state value; but, by combining the stresses with the stresses at the limit state; and considering their interactions, an ultimate value is obtained as the criterion of failure, as given in Equation (1):

$$\frac{F}{f_c} - S \geq 0 \quad (1)$$

where in, F is a function of the principal stresses state (σ_{xp} , σ_{yp} , σ_{zp}), f_c is characteristic compressive strength of masonry, S is the failure surface expressed in terms of principal stresses, and σ_{xp} , σ_{yp} , σ_{zp} are the principal stresses (in principal directions). The parameters of Willam-Warnke criterion (used in ANSYS [25]) for the masonry assemblage of clay brick and clay-gypsum mortar; were calculated from Equations (2) to (6) [27], and values for the parameters used in this study (for $f_c = 2.73$ MPa) are shown in Table 2.

$$f_t = 0.1f_c \quad (2)$$

$$f_{cb} = 1.2f_c \quad (3)$$

$$f_1 = 1.45f_c \quad (4)$$

$$f_2 = 1.725f_c \quad (5)$$

$$|\sigma_h^a| \leq 3^{0.5}f_c \quad (6)$$

where in, f_t is the uniaxial tensile strength, f_{cb} is the biaxial compressive strength, f_1 is the biaxial compressive strength for the case of hydrostatic pressure, f_2 is the uniaxial compressive strength for the case of hydrostatic pressure, $|\sigma_h^a|$ is the hydrostatic pressure, TCF is the stiffness multiplier for the cracked tensile condition, β_t is the shear transfer coefficient across the

TABLE 2. Parameters of Willam-Warnke failure criterion (used in ANSYS) [25, 29]

f_t (MPa)	0.27
f_{cb} (MPa)	3.28
f_1 (MPa)	3.96
f_2 (MPa)	4.71
$ \sigma_h^a $ (MPa)	4.73
TCF	0.6
β_t	0.15
β_c	0.75

open crack, and β_c is the shear transfer coefficient across the closed crack.

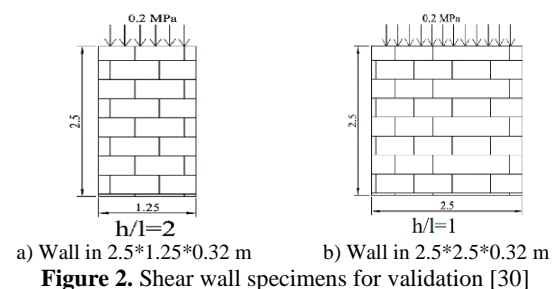
3. VALIDATION OF NUMERICAL MODELLING

To make sure about credibility of details in the way of making the walls numerical models, chosen failure criterion, assigned values for the input parameters, and also results to be obtained, initially, it is necessary to validate numerical results by the available data from the experimental specimens. This important was achieved by modelling of in-plane masonry shear walls with available experimental results [30]. This verification was performed on two wall specimens with different dimensions. The first specimen is in 250 cm height and 125 cm length (Figure 2a), and the second one is in both height and length of 250 cm (Figure 2b). The nominal thickness of the specimens is 32 cm. A constant gravity load of 0.2 MPa was applied on top of the walls, as pre-compression. The parameters of Willam-Warnke criterion was set in accordance with the available data from the experimental ones.

In Figure 3, the obtained numerical force-displacement curves were compared with the experimental ones. Due to the different number of experimental samples and easier perception, the experimental results are shown as a shading area. As shown in Figure 3, the numerical results are satisfactorily verified by the experimental ones, in their initial stiffness and the peak load. As it is shown, the numerical estimated of shear capacity reaches 86.4 kN and 223.3 kN for two specimens, which is within the limits of what achieved in experiments (grey area). Therefore, it can be concluded that further considered numerical models with the same procedure and details of modelling, failure criterion, and input data for the material parameters, will acceptably predict the real shear behavior of those real ones.

4. PARAMETRIC ANALYSIS

In this section, nonlinear pushover analyses results of 48 shear walls –similar to what were used for validation purpose- with the same details of modelling and material



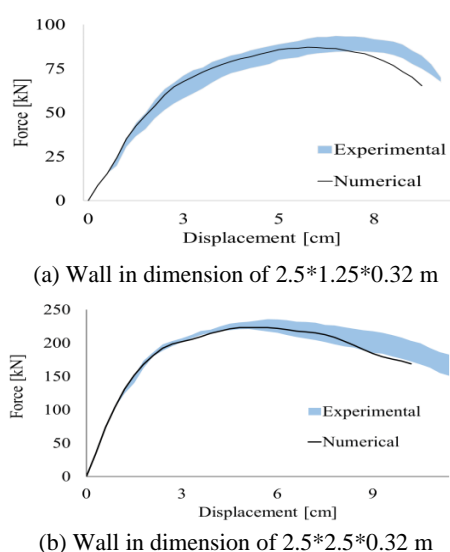


Figure 3. Comparison of the force-displacement diagrams for the validation models [31]

characteristics is presented. Behavior of the walls in distinct lateral constraints (shown in Figure 1), in height of 3.0 m and aspect ratios of 0.5, 0.75, 1.0 and 1.5, in thicknesses of 0.20, 0.35, and 0.50 m, under constant pre-compression level of 0.10 MPa, for the material characteristics (Table 2) are investigated. In all models, the top slab is in thickness of 20 cm; and the transverse walls are in the same thickness of the base shear wall, with 3.0 m length on each side of the shear wall. Figure 4 indicates the force-displacement behavioral curves for the specimens with different lateral constraints and aspect ratios; for the walls with a thickness of 0.20 m. The force-displacement curves for the specimens with an aspect ratio of 0.5 are shown in Figure 4a. In this figure, it is clear that the walls with more components of the lateral constraints had higher shear strength and less displacement capacity. The force-displacement curves of the walls with an aspect ratio of 0.75, 1.0 and 1.5 are also depicted in Figures 4b, 4c, and 4d, respectively. From the curves in Figure 4, it is apparent that the specimens with more lateral constraint components had lower ultimate displacement and higher shear strength. In addition, by increasing aspect ratio, the shear strength was reduced while the ultimate displacement was increased. It should be noted that the "H+V" wall with the aspect ratio of 0.5 and the "H" wall with the aspect ratio of 1.0 -in their post peak area- had a smaller shear strength than the specimens with lower lateral constraints, which is mainly due to the dependency of numerical results on the assumed geometric configuration and boundary conditions of the models, as well as meshing and non-real numerical parameters. Figures 5 and 6 illustrate the force-displacement curves for the specimens with 0.35 m and 0.50 m thicknesses, respectively. As it is evident,

increasing wall thickness led to higher shear strength and lower ultimate deformation. For instance, the ultimate deformations of specimens with 0.35 m and 0.50 m thicknesses are between 5.0 and 6.0 cm, while for the wall with 0.20 m thickness it is in range of 7.0 to 8.0 cm. Also, for the "H+V" wall with the aspect ratio of 0.5 -as a sample- with 20 cm thickness its shear strength is 675 kN (Figure 4a), while with 0.35 m and 0.50 m thicknesses, its shear strength is 852 kN and 1158 kN, respectively (Figures 5a and 6a).

Also, it can be concluded that the two transverse wall components were more efficient in confining and stiffening of the wall, than the top slab, which consequently affected in reduction of the ultimate displacement as well as increase in shear strength. Moreover, for a given aspect ratio, there was not significant changes in initial stiffness of the walls with distinct lateral constraints. It should be mentioned that difference in the end-point of the curves are due to the run termination by the program. To obtain the normalized ultimate displacement value, it is necessary to equate the results of these curves to idealized bilinear envelopes.

4. 1. Idealized Bilinear Envelopes

In this section, the aforementioned force-displacement curves are idealized by bilinear curves (linear elastic-perfectly plastic), to facilitate comparison objectives and driving desired numerical values. For idealization; the effective stiffness (K_{eff}), the ultimate deformation (d_u), and the normalized ultimate shear force (F_u) are the required parameters to define the bilinear curves. The modified ultimate deformation corresponds to the point with 80% reduction in the maximum shear force ($0.8 \times F_{max}$), after the peak point [31]. Figure 7 schematically illustrates the followed calculation method to extract aforementioned parameters. In more details, the effective stiffness is evaluated from the slope of the initial part of the curve up to 70% of maximum shear force ($0.7 F_{max}$), while F_{max} is the maximal shear force on the curve. Finally, by choosing the appropriate values for the normalized ultimate shear force (F_u) and drawing a horizontal line that represents perfect plastic yielding of the material, so that the area under the two curves become identical, the bilinear curve is obtained. Thus, the obtained idealized curves for investigated specimens with different lateral constraints, aspect ratios, and thicknesses are presented in Figures 8 to 10.

The linear elastic-perfectly plastic envelopes in Figure 8 is derived from the obtained responses presented in Figure 4; which were the result of specimens with thickness of 0.20 m. Ultimate deformation for the masonry walls with thickness of 0.20 m were obtained in range of 6 to 8 cm. The bilinear envelopes in Figures 9 and 10 are derived from the presented data in Figures 5 and 6; which are the result of specimens with thicknesses of 0.35 and 0.50 m, respectively. Figures 9 and 10 are

evidences of descending trend in deformation capacity (d_u) by increasing the lateral constraints components and reducing the aspect ratio.

4. 2. Ultimate Drift Values Values of ultimate relative deformation or ultimate drift representing the ratio of modified deformation capacity to the specimen height (d_u/H); are reported in Table 3. The outcomes were categorized based on lateral constraints, aspect ratio, and thickness. For an illustrating example, the results for the thickness variable are shown in Figure 11. As it can be inferred, increasing thickness of the masonry walls reduces their ultimate drift of d_u/H ; which varies in range of 1.3 to 2.6%.

4. 3. Derivation of Partial Factor Γ_{du} for Deformation Capacity under Uncertainty Conditions

Accurate modeling and input parameter estimation are significant to obtain reliable results from the actual nonlinear behavior of the structure, so, it is necessary to investigate the impact of variability on geometry and material properties. As stated, also, the three-dimensional finite element model for masonry material for both modes; the geometrical conditions and parameters of material properties; were evaluated. Two parameters are analyzed in this study, namely the modulus of elasticity and the thickness of the wall. In order to obtain a measure of uncertainty in drift capacity partial factor (γ_{du}) is proposed, somehow, deformation,

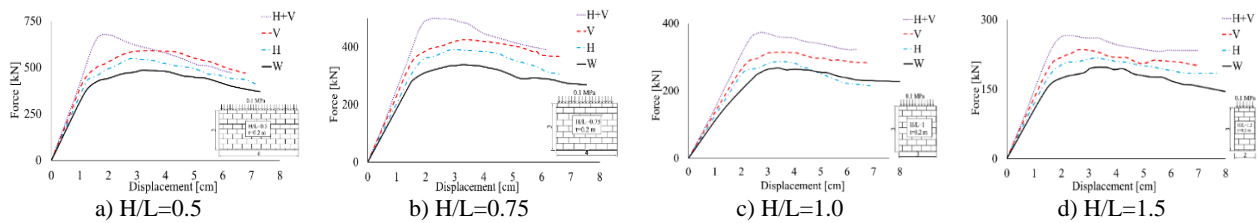


Figure 4. Force-displacement curves for masonry walls with distinct lateral constraints and aspect ratios, walls in thickness of 20cm

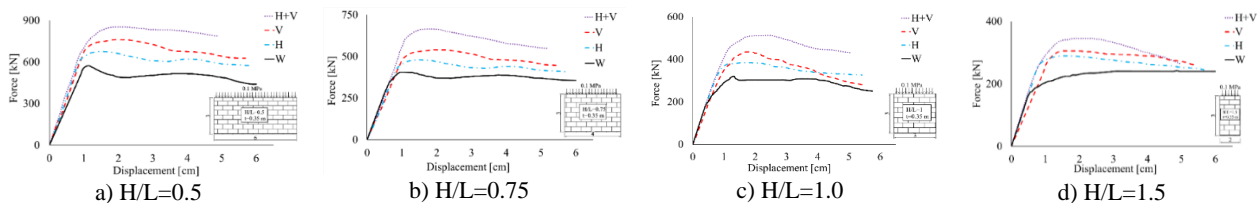


Figure 5. Force-displacement curves for masonry walls with distinct lateral constraints and aspect ratios, walls in thickness of 35cm

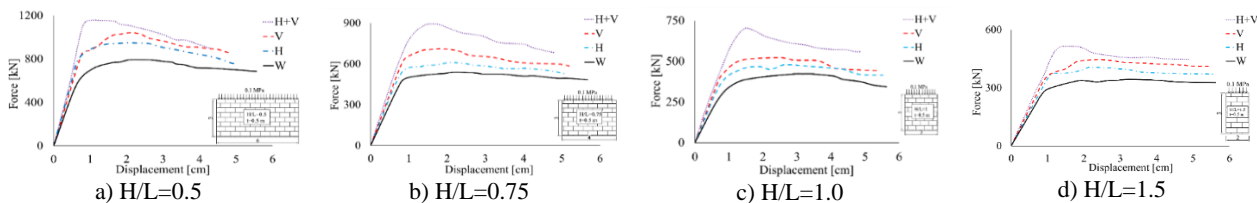


Figure 6. Force-displacement curves for masonry walls with distinct lateral constraints and aspect ratios, walls in thickness of 50cm

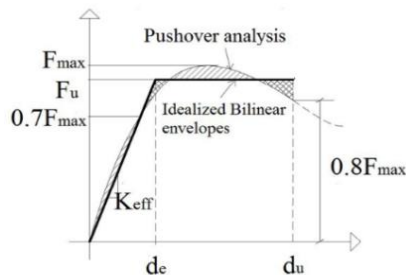


Figure 7. Definition of the parameters of the idealized bilinear envelope [31]

capacity of the wall is obtained by multiplying this factor in the modified deformation (obtained from bilinear F-d curves). In fact, to the aim of this study, the purpose of idealizing the results was to determine modified d_u characteristics (from bilinearization) to calculate the partial factor (γ_{du}). Studying the uncertainty effects was carried out using the utilities which are provided by the ANSYS program [24]. The probability distribution function of the variables (modulus of elasticity and thickness) and their covariance values are the input data given to the program.

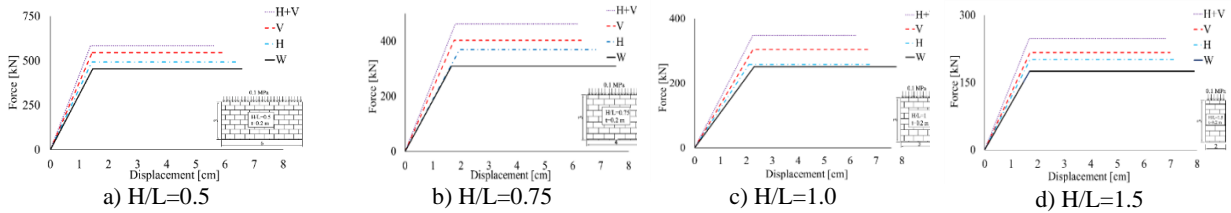


Figure 8. Idealized bilinear envelopes for masonry walls with distinct lateral constraints and aspect ratios, walls in 20cm thickness

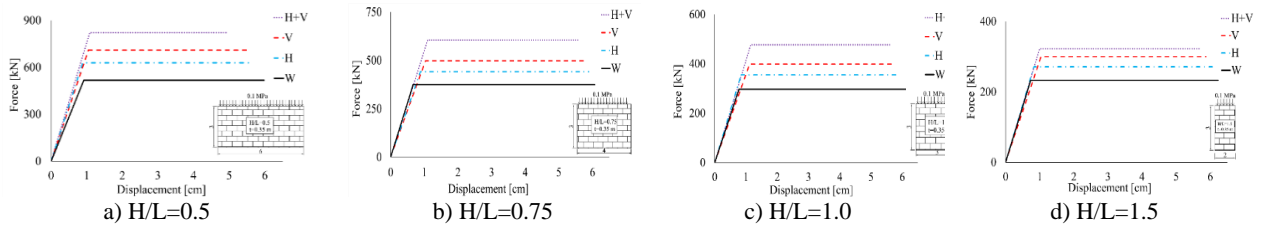


Figure 9. Idealized bilinear envelopes for masonry walls with distinct lateral constraints and aspect ratios, walls in 35cm thickness

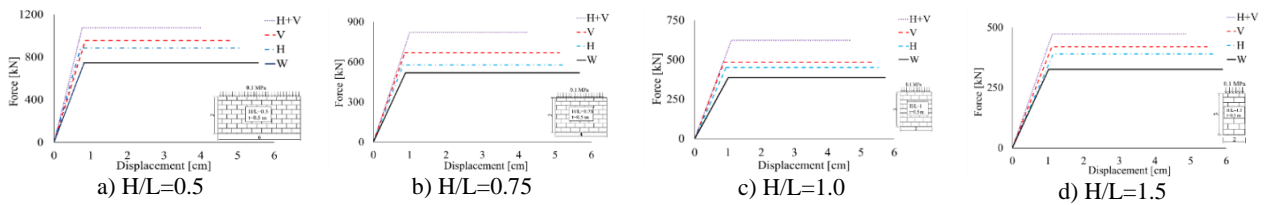


Figure 10. Idealized bilinear envelopes for masonry walls with distinct lateral constraints and aspect ratios, walls in 50cm thickness

For that purpose for each of the 48 individual studied specimens, thirty simulations were performed taking into account the consideration of modulus of elasticity and thickness; as random variables. The number of simulations (i.e. 30) was chosen so that the variation on the mean value of the response of the walls did not change more than 5% with the increase of more simulations. The force-displacement curves -which acquired from the analysis of each of the thirty specimens - were used by random variables wherein the modulus of elasticity was implemented by a log-normal probability distribution with a CoV of 0.25 [32], and the thickness was modeled by a normal probability distribution with CoV of 0.2 [33]. Then, the modified γ_{du} values for each specimen were accessed using the bilinear curves of each simulation. The partial factor (γ_{du}) for drift capacity was achieved by dividing the du/H value of the specimen without any uncertainty analysis to the du/H value obtained from the simulation of the thirty specimens with random properties. The γ_{du} value for each combination were attained according to the described procedure and summarized in Table 4 for all specimens with distinct variables.

The results in Table 4 to improve the perception of the relationships between variables in the value of the partial factor (γ_{du}) are plotted in Figure 12. From the

results in Figure 12, it can be concluded that by increasing the lateral constraint components of the wall, the value of the partial factor (γ_{du}) has decreased. In addition, by increasing the aspect ratio (height-to-length), the value of the γ_{du} factor has increased. For example, for a shear wall without any lateral constraints ("W"), with aspect ratio of 0.5 and thickness of 0.35 m, the γ_{du} value is 1.34; which is 7%, 9% and 14% smaller than the walls with aspect ratios of 0.75, 1.0 and 1.5, respectively. A similar trend can be noticed for other samples. Finally, according to Table 4, partial factor of deformation capacity (γ_{du}) for the Persian historic brick masonry was obtained between 1.3 and 1.7, depending on its lateral constraint, aspect ratio, and thickness conditions.

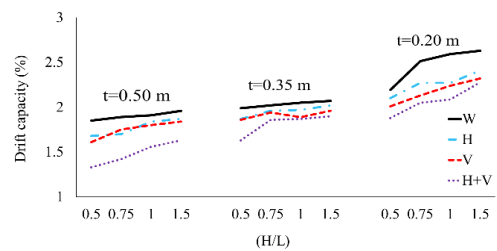


Figure 11. Ultimate drift vs. aspect ratio for the masonry walls with distinct thicknesses and lateral constraints

TABLE 3. Drift capacity values (d_u/H) for the masonry walls with distinct lateral constraints, aspect ratios, and thicknesses (in percentage)

Specimen	Lateral constraints	Wall thickness=20 cm				Wall thickness=35 cm				Wall thickness=50 cm			
		0.5	0.75	1	1.5	0.5	0.75	1	1.5	0.5	0.75	1	1.5
	H/L (aspect ratio)												
W	Original building wall	2.19	2.51	2.59	2.63	1.99	2.02	2.05	2.07	1.85	1.89	1.91	1.96
H	With top slab	2.10	2.27	2.27	2.41	1.87	1.96	1.97	2.02	1.68	1.70	1.84	1.87
V	With transverse walls on both sides	2.01	2.13	2.24	2.32	1.86	1.94	1.89	1.96	1.61	1.75	1.80	1.84
H+V	With top slab and transverse walls	1.88	2.05	2.08	2.27	1.63	1.86	1.87	1.90	1.33	1.42	1.56	1.63

TABLE 4. Partial factor γ_{du} for the masonry walls with distinct lateral constraints, aspect ratios, and thicknesses

Specimen	Lateral constraints	Wall thickness=20 cm				Wall thickness=35 cm				Wall thickness=50 cm			
		0.5	0.75	1	1.5	0.5	0.75	1	1.5	0.5	0.75	1	1.5
	H/L (aspect ratio)												
W	Original building wall	1.48	1.57	1.59	1.64	1.34	1.43	1.48	1.52	1.41	1.42	1.48	1.56
H	With top slab	1.43	1.46	1.53	1.58	1.29	1.41	1.42	1.45	1.38	1.36	1.45	1.52
V	With transverse walls on both sides	1.45	1.52	1.54	1.56	1.31	1.39	1.43	1.39	1.34	1.37	1.39	1.46
H+V	With top slab and transverse walls	1.36	1.43	1.48	1.51	1.27	1.34	1.39	1.41	1.30	1.38	1.36	1.39

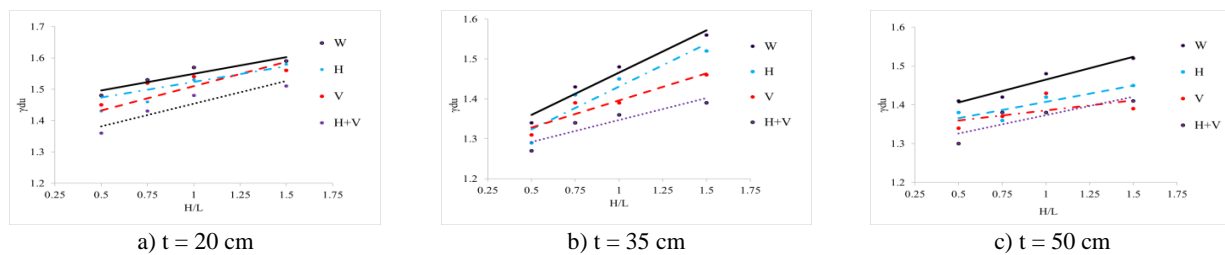


Figure 12. Partial factor γ_{du} for the masonry walls with distinct lateral constraints, aspect ratios, and thicknesses

5. SUMMARY AND CONCLUSION

In this study, it was attempted to investigate the deformation capacity for the Persian historic brick masonry under the influence of various variables under uncertainty conditions. The variety of lateral constraints, the height-to-length aspect ratio, and thickness of the wall have been investigated. For that aim, different combinations (48 different specimens) of masonry walls under in-plane loading were tested numerically in four different lateral constraints, four different height-to-length ratios, and three distinct thicknesses of the wall. The results indicated dependency of the deformation capacity to these variables. In addition, the effect of uncertainty on two parameters of modulus of elasticity (material parameter) and thickness of the specimens (geometry parameter) was investigated. As an outcome, it was tried to propose a partial factor (γ_{du}), to consider uncertainty effect in deformation capacity value (d_u), so that the deformation capacity is computed by multiplying the computed deformation capacity (d_u) by the (γ_{du}).

1. It was determined that increasing in lateral constraint components, and thickness of the wall, caused decrease in deformation capacity (d_u) of the wall.
2. The wall deformation capacity (d_u) increased by increasing its aspect ratio.
3. Evaluation to examine the effect of vertical and horizontal constraints, separately, showed that the effect of two vertical constraints (transverse walls at two ends and on both sides) on reduction of the wall drift capacity was more than the top slab.
4. Based on these numerical computations, the ultimate drift value of d_u/H ; for the shear walls with Persian historic material, obtained in range of 1.3 to 2.6%.
5. The results showed that by increasing lateral constraint components, and wall thickness, in contrary to the aspect ratio, the value of partial factors (γ_{du}) for deformation capacity was decreased.
6. The value of the partial factors for the wall deformation capacity (γ_{du}) based on the considered conditions in this study, is proposed in range of 1.3 to 1.7.

It was tried to delimit the results of this study only on specific governed conditions, assumptions and limitations including; walls typology, aspect ratio, thickness, protocols on numerical modelling and bilinearization technique, the method and parameters used in uncertainty studying, and especially the Persian historic masonry material properties. Definitely, to increase reliability on the results, it should study quite more experimentals as well as numerical specimens, with different conditions of historic masonry structures..

Finally, it should be mentioned that in cases of design purposes, the proposed values for (γ_{du}) should be magnified, by dividing γ_{du} on a less than one factor (This is an adaptation from the codes in computing the partial safety factor for materials (γ_M), using factor of 0.8).

6. REFERENCES

- Hamid, A.A., Mahmoud, A. and El Magd, S.A., "Strengthening and repair of unreinforced masonry structures: State-of-the-art", in Proc., 10th Int. Brick and Block Masonry Conf. Vol. 2, (1994), 485-497. DOI: 10.1061/(ASCE)1090-0268(2001)5:2(76)
- Salmanpour, A.H., Mojsilović, N. and Schwartz, J., "Displacement capacity of contemporary unreinforced masonry walls: An experimental study", *Engineering Structures*, Vol. 89, (2015), 1-16. DOI:10.1016/j.engstruct.2015.01.052
- Feba, S.T. and Kuriakose, B., "Nonlinear finite element analysis of unreinforced masonry walls", in Applied Mechanics and Materials, Trans Tech Publ. Vol. 857, (2017), 142-147. DOI: 10.4028/www.scientific.net/AMM.857.142
- Hendry, A., Samarasinghe, W., Page, A. And Poisson, "A finite element model for the in-plane behaviour of brickwork", *Proceedings of the Institution of Civil Engineers*, Vol. 73, No. 1, (1982), 171-178. DOI: 10.1680/iicep.1982.1878
- Laurenco, P., Rots, J.G. and Blaauwendraad, J., "Two approaches for the analysis of masonry structures: Micro and macro-modeling", *HERON*, Vol. 40, No. 4, (1995). <http://resolver.tudelft.nl/uuid:c39b29ab-3c75-47db-9cb5-bf2b1c678f1f> [Accessed 01. 01. 1995]
- Najafgholipour, M., Maheri, M.R. and Lourenço, P.B., "Capacity interaction in brick masonry under simultaneous in-plane and out-of-plane loads", *Construction and Building Materials*, Vol. 38, (2013), 619-626. DOI:10.1016/j.conbuildmat.2012.08.032Get rights and content
- Niasar, A.N., Alaei, F.J. and Zamani, S.M., "Experimental investigation on the performance of unreinforced masonry wall, retrofitted using engineered cementitious composites", *Construction and Building Materials*, Vol. 239, (2020), 117788. DOI: 10.1016/j.conbuildmat.2019.117788
- Howlader, M., Masia, M. and Griffith, M., "Numerical analysis and parametric study of unreinforced masonry walls with arch openings under lateral in-plane loading", *Engineering Structures*, Vol. 208, (2020), 110337. DOI: 10.1016/j.engstruct.2020.110337
- Howlader, M., Masia, M. and Griffith, M., "In-plane shear testing of unreinforced masonry walls and comparison with fea and nzsee predictions", *International Journal of Masonry Research and Innovation*, Vol. 5, No. 1, (2020), 47-66. DOI: 10.1504/IJMRI.2020.104845
- Roca, P., "Assessment of masonry shear-walls by simple equilibrium models", *Construction and Building Materials*, Vol. 20, No. 4, (2006), 229-238. DOI: 10.1016/j.conbuildmat.2005.08.023
- Giordano, A., De Luca, A., Mele, E. and Romano, A., "A simple formula for predicting the horizontal capacity of masonry portal frames", *Engineering Structures*, Vol. 29, No. 9, (2007), 2109-2123. DOI: 10.1016/j.engstruct.2006.10.011
- Howlader, M., Masia, M. and Griffith, M., "In-plane response of perforated unreinforced masonry walls under cyclic loading: Experimental study", *Journal of Structural Engineering*, Vol. 146, No. 6, (2020), 04020106. DOI: 10.1061/(ASCE)ST.1943-541X.0002657
- Moon, F.L., "Seismic strengthening of low-rise unreinforced masonry structures with flexible diaphragms", Georgia Institute of Technology, (2003), <http://hdl.handle.net/1853/5128>
- Engineering, N.Z.S.f.E., "Assessment and improvement of the structural performance of buildings in earthquakes: Prioritisation, initial evaluation, detailed assessment, improvement measures: Recommendations of a nzsee study group on earthquake risk buildings, New Zealand Society for Earthquake Engineering, (2014). <https://www.nzsee.org.nz/library/guidelines/>
- Yi, T., "Experimental investigation and numerical simulation of an unreinforced masonry structure with flexible diaphragms", Georgia Institute of Technology, (2004), <http://hdl.handle.net/1853/5149>
- Choudhury, T. and Kaushik, H.B., "Influence of individual wall strengths on lateral strength of urm buildings constructed using low-strength masonry", *Journal of Earthquake Engineering*, (2020), 1-28. DOI: 10.1080/13632469.2020.1742253
- Standard, B., "Eurocode 6—design of masonry structures—", British Standard Institution. London, Vol., No., (2005).
- Code, P., "Eurocode 8: Design of structures for earthquake resistance-part 1: General rules, seismic actions and rules for buildings", Brussels: European Committee for Standardization, (2005).
- Council, A.T. and Response, P.f., "Evaluation of earthquake damaged concrete and masonry wall buildings: Basic procedures manual, The Agency, (1999).
- Council, B.S.S., "Nehrp guidelines for the seismic rehabilitation of buildings", FEMA-273, Federal Emergency Management Agency, Washington, DC, (1997), 2-12.
- SIA, S., "266: Masonry", Swiss code, Swiss society of engineers and architects SIA, Zürich, Switzerland, (2005).
- ASCE, Fema 356-prestandard and commentary for the seismic rehabilitation of buildings. 2000.
- Petry, S. and Beyer, K., "Influence of boundary conditions and size effect on the drift capacity of urm walls", *Engineering Structures*, Vol. 65, (2014), 76-88. DOI: 10.1016/j.engstruct.2014.01.048
- Tomažević, M. and Weiss, P., "Displacement capacity of masonry buildings as a basis for the assessment of behavior factor: An experimental study", *Bulletin of Earthquake Engineering*, Vol. 8, No. 6, (2010), 1267-1294. DOI: 10.1007/s10518-010-9181-y
- ANSYS, A., 14, *ansys inc., basic analysis procedures guide release 14*.
- Hejazi, M.M. and Saradj, F.M., "Persian architectural heritage: Structure, WIT Press, (2014).
- Binda, L., Fontana, A. and Frigerio, G., "Mechanical behaviour of brick masonries derived from unit and mortar characteristics", Brick and Block Masonry (8 th IBMAC) London, Elsevier Applied Science, Vol. 1, (1988), 205-216. <http://www.hms.civil.uminho.pt/ibmac/1988/205.pdf>
- D'Altri, A.M., Sarhosis, V., Milani, G., Rots, J., Cattari, S., Lagomarsino, S., Sacco, E., Tralli, A., Castellazzi, G. and de Miranda, S., "Modeling strategies for the computational analysis

- of unreinforced masonry structures: Review and classification", *Archives of Computational Methods in Engineering*, (2019), 1-33. DOI: 10.1007/s11831-019-09351-x
29. Drobiec, L. and Jasiński, R., "Adoption of the willam-warnke failure criterion for describing behavior of ca-si hollow blocks", *Procedia Engineering*, Vol. 193, (2017), 470-477. DOI: 10.1016/j.proeng.2017.06.239
30. Magenes, G., Galasco, A., Penna, A. and Da Paré, M., "In-plane cyclic shear tests of undressed double leaf stone masonry panels", in Proceedings of the 14th European conference on earthquake engineering. Ohrid. (2010). <https://www.masonry.org.uk/downloads/volume-1-d-216>
31. Tomaževič, M., "Earthquake-resistant design of masonry buildings, World Scientific, (1999).
32. Code, J.P.M., "Joint committee on structural safety", URL: www.jess.ethz.ch, (2001).
33. Zhai, X. and Stewart, M., "Structural reliability of reinforced concrete block masonry walls in concentric compression", in 11th Canadian Masonry Symposium. Vol. 32, No. 1, (2009). DOI: 10.1016/j.engstruct.2009.08.020

Persian Abstract

چکیده

در اکثر آیین‌نامه‌های سازه‌ای، ظرفیت جابجایی در دیوارهای برشی بنایی، تخمینی از عملکرد رفتاری (و نوع شکست) و نسبت ابعادی ارتفاع به طول نمونه‌ها می‌باشد. این تحقیق، به منظور بررسی ظرفیت جابجایی دیوارهای برشی بنایی تاریخی ایرانی تحت تاثیر پارامترهایی نظیر قیودات جانبی، نسبت ابعادی و ضخامت دیوار انجام شده است. همچنین، برای مدل‌کردن اثر عدم قطعیت در مصالح و هندسه دیوار، ضریب جزئی γ_{du} پیشنهاد گردید، بطوریکه، جابجایی نهایی دیوار از حاصلضرب تغییر مکان محاسباتی در این ضریب جزئی بدست می‌آید. از این رو، ۴۸ نمونه مختلف از دیوارهای بنایی تحت بارگذاری برشی درون‌صفحه‌ای، برای چهار حالت مختلف از قیودات جانبی (ناشی از اثرات دیوارهای جانبی و سقف)، چهار نسبت ابعادی ارتفاع به طول ۰/۵، ۰/۷۵، ۱، و ۱/۵، با سه اندازه مرسوم برای ضخامت دیوار (۰/۲، ۰/۳۵، و ۰/۵ متر)، تحت بار پیش فشار ۰/۱ مگاپاسکال (متناظر بار یک سقف) مدل‌سازی گردیدند. پس از تهیه منحنی‌های رفتاری بار-تغییر مکان (منحنی ظرفیت)، به منظور ساده‌سازی پاسخ‌ها و نیز کاربردی‌تر کردن آنها، ایده‌آل‌سازی نتایج توسط منحنی‌های دوخطی الاستیک خطی-پلاستیک کامل، انجام گردید. نتایج ناشی از ایده‌آل‌سازی منحنی‌های رفتاری بار-تغییر مکان، مشخص نمود که با افزایش قیودات جانبی، افزایش ضخامت، و نیز کاهش نسبت ابعادی؛ ظرفیت جابجایی دیوارهای بنایی کاهش می‌یابد. ضمناً، مشاهده گردید که قید جانبی دیوارهای عرضی - اتصال‌یافته در هر دو انتها و در هر دو طرف دیوار برشی - نسبت به مولفه‌ی افقی (سقف تنها) در کاهش ظرفیت جابجایی و افزایش سختی دیوار برشی موثرتر می‌باشد. بر اساس این مدل‌سازی‌ها، نسبت تغییر مکان جانبی نهایی به ارتفاع (دریفت نهایی) برای دیوارهای برشی بنایی تاریخی ایرانی در بازه ۱/۳ تا ۲/۷ درصد بدست آمد. در نهایت، ضریب جزئی γ_{du} برای لحاظ نمودن عدم قطعیت در برآورد دو پارامتر مدول الاستیسیته مصالح و ضخامت دیوار در تعیین دریفت نهایی دیوار برشی با مصالح بنایی تاریخی ایرانی؛ در بازه ۱/۳ تا ۱/۷ حاصل گردید.
